Immunology Letters 122 (2009) 159–169

Contents lists available at ScienceDirect

Immunology Letters

journal homepage: www.elsevier.com/locate/

The drug monosodium luminol (GVT®) preserves thymic epithelial cell cytoarchitecture and allows thymocyte survival in mice infected with the T cell-tropic, cytopathic retrovirus *ts*1

Virginia L. Scofield*, Mingshan Yan, Xianghong Kuang, Soo-Jin Kim, Derek Crunk, Paul K.Y. Wong

Department of Carcinogenesis, The University of Texas M.D. Anderson Cancer Center, Science Park - Research Division, 1808 Park Road 1-C, Smithville, TX 78957, USA

ARTICLE INFO

Article history:
Received 25 July 2008
Received in revised form
14 November 2008
Accepted 1 December 2008
Available online 23 February 2009

Keywords:
GVT
Thymus
Oxidative stress

ABSTRACT

A mutant of MoMuLV, called *ts*1, causes an AIDS-like syndrome in susceptible strains of mice. In mice infected at birth, thymic atrophy, CD4+ T cell loss, body wasting, and death occur by ~30–40 days postinfection (dpi). We have shown previously that the death of *ts*1-infected cells is not caused by viral replication *per se*, but by oxidative stress and apoptosis following their accumulation the *ts*1 viral envelope precursor protein, gPr80^{env}. In infected mice treated with the antioxidant monosodium α-luminol (GVT®), T cell loss and thymic atrophy are delayed for many weeks, and body wasting and death do not occur until long after infected, untreated control mice have died. We show here that GVT treatment of *ts*1-infected mice maintains the thymic epithelial cell (TEC) cytoarchitecture and cytokeratin gradients required for thymocyte differentiation. It also suppresses thymocyte reactive oxygen species (ROS) levels, upregulates and stabilizes levels of the antioxidant-regulating transcription factor Nrf2, and prevents accumulation of gPr80^{env} in thymocytes. We conclude that GVT treatment can make *ts*1 a non-cytopathic virus for thymocytes, although it cannot prevent thymocyte infection. Since oxidative stress also contributes to the loss of T cells in HIV-AIDS, the antioxidant effects of GVT may make it a useful therapeutic adjunct to HAART treatment.

1. Introduction

The known T cell-tropic retroviruses of vertebrates include Type C or D retroviruses and many lentiviruses [1–4]. Some of these agents cause leukemias and lymphomas after a months-long latent period in their host species, while others cause fulminant diseases that lead to death within weeks of infection. Interestingly, although HIV-1 and the lentivirus simian immunodeficiency virus (SIV) use CD4 as their surface receptor on T cells, other T cell-tropic retroviruses do not [5–7]. Despite this, thymic atrophy, selective infection and killing of CD4+ T-lineage cells, or neoplastic transformation of thymocytes, are common characteristics of diseases caused by these viral agents [8–14]. At present, the cause of T cell death after infection by these viruses is unknown.

In this laboratory, we study the T cell-tropic retrovirus *ts*1, which is a mutant of Moloney murine leukemia virus-TB (MoMuLV) [15,16]. Because of the disease it causes, this agent falls into the group of acute cytopathic retroviruses identified above, although its parent strain MoMuLV-TB has a long latent period, and, like other long-latency leukemia viruses, it causes T cell neoplasia rather than T cell death. When used to infect newborn mice of susceptible strains, the *ts*1 virus induces a neurodegenerative and immunosuppressive syndrome with many features in common with HIV-AIDS [17–21]. During its short disease course, *ts*1 selectively infects and kills peripheral CD4+ T cells [19,20,22,23], although its receptor on T cells is not CD4, but instead is the cationic amino acid receptor MCAT-1 [5]. This CD4+ T cell loss leads rapidly to immunodeficiency, wasting and death [24]. If infection is delayed for days or weeks after birth, or if lower virus doses are used to infect newborn pups, the latent period to disease can be prolonged by many months, although the disease, once it develops, has a rapid course similar to that caused earlier by higher doses of *ts*1 [25].

*ts*1 disease resembles HIV-AIDS in its latency-period spectrum. In the pre-HAART era of the HIV-AIDS epidemic, some infected individuals developed full-blown disease and died within weeks or months of primary infection, while other patients did not develop disease for years [2]. One reason for this, for both viruses, may involve a role for genetics in susceptibility to infection. Some inbred mouse strains are completely resistant to *ts*1 infection (e.g., C57Bl/6), while others are very susceptible, as is our index strain FVB/N [15]. We suspect that the reliable and

* Corresponding author at: Department of Carcinogenesis, The University of Texas M.D. Anderson Cancer Center, Science Park - Research Division, PO Box 389, Smithville, TX 78957, USA. Tel.: +1 512 237 9344; fax: +1 512 237 2444.
E-mail address: vscofield@mdanderson.org (V.L. Scofield).

0165-2478/$ – see front matter © 2009 Elsevier B.V. All rights reserved.
doi:10.1016/j.imlet.2008.12.009

short timeline for *ts*1 disease is due to our use of FVB/N mice for infection, our use of a standard virus dose that kills the animals by 30–40 dpi, and the young age of the animals when infected (at birth).

In CNS astrocytes and thymocytes infected with *ts*1, inefficient cleavage of the viral envelope preprotein $gPr80^{env}$ causes it to accumulate in infected cells [26–28]. In cell types that process $gPr80^{env}$ normally (yielding the two mature envelope proteins gp70 and PrP15E), *ts*1 infection does not cause cell death. In cell types that do die after *ts*1 infection, accumulated $gPr80^{env}$ initiates an unfolded protein response (UPR), which in turn causes endoplasmic reticulum (ER) stress. The result is release of Ca^{2+} from cytoplasmic stores, obligatory loading of this Ca^{2+} into mitochondria, mitochondrial stress, and finally by profound oxidative stress, leading to apoptosis [29–39]. Together our findings show that *ts*1-infected target cells, which include astrocytes, thymocytes and CD4+ T cells, are not killed by virus infection per se, but instead die by apoptosis caused by oxidative stress [23–29].

Oxidative stress occurs in cells when the production of reactive oxygen species (ROS) exceeds antioxidant defenses [40]. At low concentrations, ROS participate in cell signaling and stimulate cell proliferation [41,42], but higher concentrations damage biomolecules in the cell, leading to depletion of reduced thiols, including the cell's major antioxidant, glutathione (GSH) [42]. Cellular defense responses to oxidative stress occur in a controlled sequence [42]. Level 1 defenses involve upregulation of superoxide dismutases and catalase, which counter the buildup of H_2O_2 formed after production of superoxide. If the ROS overload overcomes these defenses, the level 2 defenses are deployed to counteract the depletion of cysteine (a GSH precursor) and GSH that follows a larger ROS challenge. At this time, the transcription factor NF-E2 related factor 2, or Nrf2, is activated [43]. Nrf2 is the central regulatory element controlling the transcription of level 2 cytoprotective genes, via the antioxidant response element (ARE) sequences in their promoter regions [43,44].

In this study, we have renewed our earlier work on the lymphoid system in the *ts*1-infected mouse. However, we have switched our focus from the peripheral lymphoid system to the thymus, and to oxidative stress mechanisms and treatments that cause or prevent thymocyte death after *ts*1 infection. We chose this emphasis because the normal mammalian thymus is the only source of naïve T cells, which it provides throughout life [45,46]. In HIV-AIDS patients, naïve T cells are necessary for generation of immune responses against new variants of HIV-1 as they arise during the disease course. Their exhaustion has been proposed as a primary mechanism for immunosuppression in HIV-AIDS [9,47]. As noted above, we still have a limited understanding of how the thymus and thymocytes are killed by cytopathic retroviruses, regardless of the virus type or species involved [10].

This work was initiated with two objectives: first, to find out how *ts*1 infection affects the thymi and thymocytes of mice, and, second, to determine how a selected antioxidant compound protects them. We have reported recently that the antioxidant compound monosodium luminol (trade name GVT®) significantly delays thymic atrophy, wasting, and death in *ts*1-infected mice, even though the thymi of GVT-treated mice contain replicating *ts*1 [29]. In *ts*1-infected mice (*ts*1-only), we report here that the epithelial cell infrastructure of the thymus is destroyed, that its thymocytes are lost to apoptosis, and that this apoptosis is accompanied by accumulation of $gPr80^{env}$. In infected mice treated with GVT (*ts*1-GVT), the epithelial cell infrastructure is maintained and the thymocytes remain alive, although they are still infected. This protective effect is associated with marked reduction in thymocyte ROS levels, upregulation and stabilization of the antioxidant transcription factor Nrf2 in the thymic epithelial cells (TECs), and lack of accumulated $gPr80^{env}$ in the thymocytes.

2. Materials and methods

2.1. Virus

The *ts*1 virus, a mutant of MoMuLV, was propagated in TB cells, a thymus-bone marrow cell line, and titered on 15F cells, as previously described [15].

2.2. Antibodies and reagents

GVT® (monosodium luminol) was provided by Bach-Pharma, Inc., North Andover, MA. Goat anti-MoMuLV gp70 was from Microbiology Associates, Burlingame, CA. This antibody recognizes epitopes shared by the mature gp70 viral envelope protein and the precursor preprotein $gPr80^{env}$. Monoclonal rabbit anti-cleaved caspase-3 was from Cell Signaling (Boston, MA). Mouse monoclonal anti-Nrf2 was from R&D systems (Minneapolis, MN). Polyclonal anticytokeratin-5 (CK5) and monoclonal anti-cytokeratin-8 (CK8) antibodies were from Covance Research (Richmond, CA) and the National Institutes of Health Developmental Studies Hybridoma Bank (Iowa City, IA), respectively. FITC and Texas Red conjugated anti-mouse, rat, rabbit and goat antibodies were from Jackson ImmunoResearch (West Grove, PA).

2.3. Measurement of intracellular ROS (H_2O_2) using DCFDA

5 (and 6)-chloromethyl-2′,7′-dichlorodihydrofluorescein diacetate (CM-H2DCFDA; Molecular Probes, Eugene, OR; hereafter called DCFDA), is a cell-permeant indicator for intracellular ROS, including hydrogen peroxide and superoxide. The dye itself is non-fluorescent, but when its acetate groups are removed by intracellular esterases, it is oxidized to form a highly fluorescent derivative, carboxydichlorofluorescein [29]. Freshly isolated thymocytes were prepared from uninfected, GVT-only, *ts*1-only and *ts*1-GVT-treated mice, at 30 dpi. The thymocytes were incubated with 10 μM of DCFDA, in culture medium (RPMI 1640) at 37 °C for 30 min. After this loading period, the cells were washed twice with PBS, and the fluorescence of their cells measured using a Synergy HT multidetection microplate reader (BioTek Instruments, Inc., Winoski, VT). The data are expressed as means ± standard deviation (SD) of relative fluorescence units for DCFDA-loaded thymocyte lysates for three mice of each treatment group.

2.4. Mice, infection, and drug treatment

FVB/N mice were obtained from Taconic Farms (Germantown, NY). Breeding FVB/N pairs were housed in sterilized microisolator cages and supplied with autoclaved feed and water *ad libitum*. The microisolators were kept in an environmentally controlled isolation room. For *ts*1 infection, 2-day-old mice were inoculated intraperitoneally with 0.1 ml of vehicle (mock infection) or with 0.1 ml of a *ts*1 suspension containing 2×10^7 infectious units/ml. Mice infected by this protocol, and at this virus dose, become paralyzed and die at 30–40 dpi.

For GVT treatment, infected mice were divided into two groups each on the day of infection. Infected mice were then divided again into two groups, one of whose individuals received 0.9% normal saline, intraperitoneally, for five continuous days a week, followed by two resting days, until the end of the experiment, while the other half of the infected animals received freshly prepared GVT, delivered intraperitoneally at 200 mg/kg body weight/day in 0.9% normal saline. The uninfected mice were also divided into two groups, one receiving saline alone, and the other receiving GVT as described above. No toxic effects are observed at any time at this dose of GVT when it is used without infection [29]. All mice were

observed daily for clinical signs of disease, and the mice from all groups were sacrificed at 30 dpi.

Whole thymi that were to be used for Western blotting were removed, snap-frozen in liquid nitrogen and stored at −80 °C until use. For immunohistochemistry, thymi were snap-frozen in liquid nitrogen in Optimal Cutting Temperature (OCT) embedding compound (Sakura Finetek USA, Torrance, CA). These experimental protocols were approved by The University of Texas M.D. Anderson Cancer Center's Institutional Animal Care and Use Committee.

2.5. Western blotting

Western blotting analysis was performed as described previously [29]. Briefly, proteins from whole thymic tissue or from isolated thymocytes were extracted with radioimmunoprecipitation assay buffer (1% NP40, 0.5% sodium deoxycholate, 0.1% sodium dodecyl sulfate, 0.25 mM phenylmethylsulfonylfluoride, 1 mg/ml aprotinin, leupeptin, and pepstatin A, 1 mM sodium orthovanadate, and 1 mM sodium fluoride in phosphate-buffered saline, or PBS). Protein concentrations were measured using Bio-Rad *D*c protein assay reagent (Bio-Rad Laboratories, Hercules, CA) as per the manufacturer's instructions.

The lysates (30 μg total protein per sample) were electrophoresed on 10% SDS-PAGE gels, and then transferred to polyvinylidene difluoride membranes (Millipore Corp, Bedford, MA). The membranes were blocked at room temperature for 1 h in Tris-buffered saline, or TBS, with 5% non-fat milk, and incubated with unconjugated primary antibodies for 2 h, followed by 3 washes with TBS. The blots were then incubated with horseradish peroxidase-conjugated secondary antibody for an additional 1 h. After three washes, immune complexes were detected by chemiluminescence (NEN Life Science Products, Boston, MA). A monoclonal anti-β-actin antibody (Sigma, St. Louis, MO) was used as a loading control. In Western blots for which fold differences of bands were calculated, the densitometry readings for the bands were first normalized against the β-actin densities for the same lanes, and then the ratio obtained from this calculation set as 1 for bands for cells or tissues from uninfected mice, and the other values calculated as the ratio of their normalized values against this number.

2.6. Immunohistochemistry

Dissected tissues were snap-frozen in OCT medium and kept at −80 °C prior to cutting of 5-μm-thick serial frozen sections. The sections were placed on microscope slides, and the slides kept at −80 °C prior to staining. For staining, the sections were thawed at room temperature for 30 min, fixed in ice-cold acetone for 5 min, washed, and incubated overnight at 4 °C with optimum dilutions of primary antibodies. The slides were then washed and incubated in FITC-conjugated or TxR-conjugated anti-rabbit, anti-rat, or anti-goat IgG Fab′2.

Where double immunostaining was done, it was with polyclonal or monoclonal antibodies raised in cells or animals from two different species, followed by FITC-conjugated anti-IgG for one species, and TxR-conjugated anti-IgG for the other. After incubation in the secondary reagents and washing, the sections were mounted in mounting medium (Vector Laboratories, Burlingame, CA) for viewing under an Olympus fluorescence microscope. Control sections were incubated (a) in affinity-purified goat, rabbit or rat IgG, depending upon the host species of the primary antibody, (b) with appropriate isotype controls, for monoclonal antibodies, (c) in secondary antibodies alone, without primary reagents. Optimum staining conditions were developed for each antibody, so that no specific binding was observed in sections incubated in control reagents, while specific binding was observed with the primary antibodies under test.

2.7. Statistical analysis

Western blotting experiments were repeated at least three times, and immunostaining studies were repeated at least twice, to verify reproducibility of results. Quantitative differences between groups in graph-displayed data were compared for statistical significance by Student's *t*-test, and *p*-values of less than 0.05 were considered statistically significant.

3. Results

3.1. Epithelial cell organization is disrupted in the thymi of *ts*1-infected mice, but maintained in infected mice treated with GVT

In the normal mouse thymus, the epithelial matrix of the organ is divided into grape-like lobules, each of which is composed of a well-demarcated outer cortical epithelium and an inner medullary epithelial cell area. Both areas are like epithelial cell "baskets" filled with thymocytes and other cell types, including macrophages, dendritic cells, fibroblasts, and a rich connective tissue matrix. In each lobule, T cell precursors arrive in the thymus from the bone marrow, landing in the corticomedullary junction (CMJ) between the cortex and medulla [48]. The subsequent differentiation of the T cell precursors into mature T cells then occurs in the context of this corticomedullary structure, during which time the thymocytes travel from the CMJ through the cortex to the outer edge of the lobule, and then come back again, all the while undergoing a scheduled differentiation sequence that takes them through defined developmental checkpoints. These events are governed by contact-mediated and humoral reciprocal crosstalk between the TECs and thymocytes [49,50].

The epithelial thymus contains two distinct kinds of cells: a simple epithelium in the cortex, and a basal epithelium in the medulla. Normal corticomedullary organization of the murine thymus has a molecular component that can be assessed using antibodies to cytokeratin markers. Cytokeratins are a diverse family of intermediate filament proteins that distinguish different epithelial cell types, including the two epithelial cell types in the mouse thymus. In the healthy mouse, the cortical epithelial cells express cytokeratin-8 (CK8), the medullary epithelial cells express cytokeratin-5 (CK5), and a small population separating in the CMJ expresses both [49]. The presence of an intact epithelial cell cytokeratin CK8/5 expression gradient, and of a clear corticomedullary boundary in H&E-stained slides, is a precise anatomical correlate of normal thymocyte differentiation [49,50].

In the mouse thymus, TEC differentiation is dysregulated if the thymocytes cannot differentiate; likewise, normal thymocytes cannot differentiate in thymi whose epithelium is abnormal (reviewed in [49]). To determine how *ts*1 infection affects the epithelial and thymocyte compartments in the thymus, and to follow GVT effects on these events, we first compared cytoarchitecture and cytokeratin expression patterns for TECs and thymocytes in uninfected, *ts*1-infected (*ts*1-only) and infected GVT-treated (*ts*1-GVT) mice sacrificed at 30 dpi. Frozen sections from thymi of uninfected and *ts*1-infected (*ts*1-only) and *ts*1-infected, GVT-treated (*ts*1-GVT) mice were prepared at 30 dpi, and then (1) stained with H&E, (2) doubly immunostained either with anti-CK8 and anti-CK5 (on an uninfected thymus section), or (3) doubly stained with anti-gp70 and CK8 (infected *ts*1-only or *ts*1-GVT thymic sections). The left side panel in Fig. 1(A) is an H&E-stained section of thymus from an uninfected mouse. It shows clear lobular cortimedullary epithelial organization, and the left immunostained section in Fig. 1(B), which also is from an uninfected mouse thymus, shows correct epithelial cytokeratin organization (CK8-positive cortex, CK5-positive

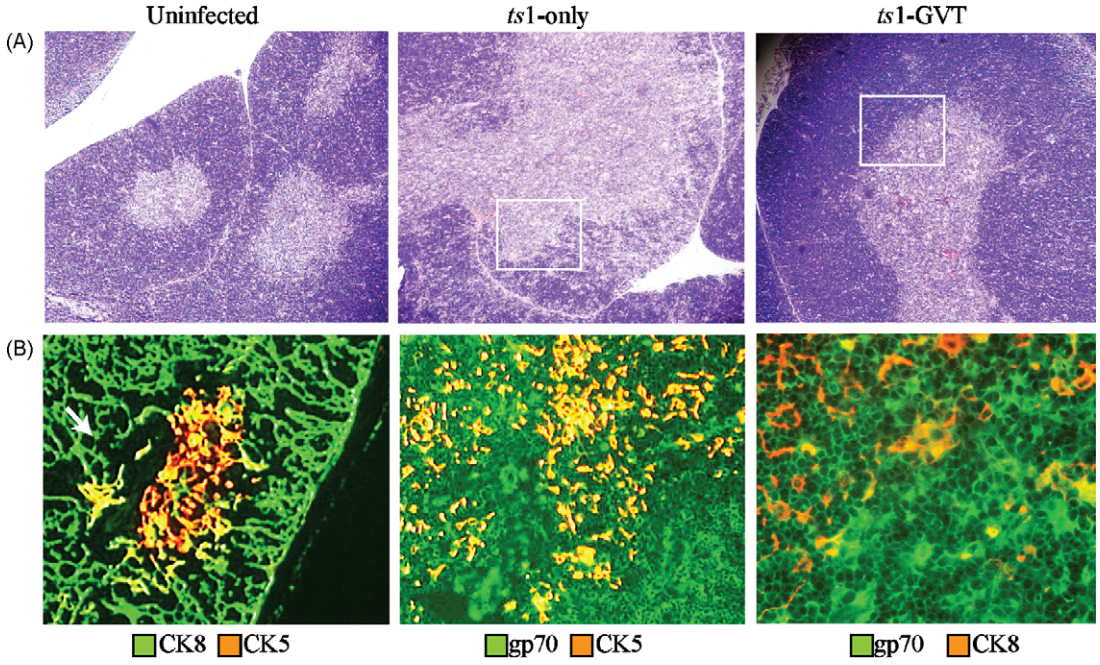

Fig. 1. Corticomedullary epithelial organization and distribution of epithelial cell cytokeratins are dysregulated in 30 dpi *ts*1-only mice, but these disturbances are prevented in *ts*1-GVT mice. The white boxes in the *ts*1-only and *ts*1-GVT H&E-stained sections in (A) correspond to the immunostained sections below them in (B). The uninfected thymus section at the left in (A) shows three lobules with normal corticomedullary organization, while the lobule in the *ts*1-only thymus section has disorganized corticomedullary organization, with a medullary epithelium whose cells have spread into the cortical subcapsular space. By contrast, the section from the *ts*1-GVT mouse thymus shows normal corticomedullary organization. The uninfected immunostained thymic lobule at the left in (B) has normal corticomedullary cytokeratin organization, in which cortical epithelial cells are CK8-positive (green), medullary epithelial cells are CK5-positive (red/orange) and the epithelial cells of the CMJ are positive for both (yellow cells; arrow). The *ts*1-only, gp70/CK5-immunostained section at the center in (B) contains infected, gp70-positive thymocytes (green) and infected, gp70-positive and CK5-positive epithelial cells (yellow). As in the *ts*1-only H&E section above in (A), the medullary epithelial cells appear to be expanding out of the medullary space, and no distinct CMJ is evident. From their uniform staining with both antibodies, all of these epithelial cells appear to be infected. The *ts*1-GVT gp70/CK8-immunostained section at the right in (B) contains infected, gp70-positive thymocytes and CK8-positive cortical epithelial cells. Some of the CK8-positive cells are also gp70-positive, by their yellow co-staining), but most appear to be singly CK8-positive, and thus may not be infected. This section also has a clearly demarcated CMJ (separating the lower right of panel from the upper left). Original magnifications: (A) all panels 4×; (B) left panel, 4×; middle panel, 10×; right panel, 20×.

medulla). In the *ts*1-only sections in the middle panel of Fig. 1(A), severe cortical thinning is evident in the H&E-stained section, and the corresponding immunostained section in Fig. 1(B) (see box in H&E section) shows that CK5-positive medullary epithelial cells are not confined to the medulla as they are in the normal thymus, but instead are growing out into the thinning thymic cortex. Fig. 1(A) and (B) also show sections from the thymic cortex of a 30 dpi *ts*1-GVT mouse (right). The H&E stained section has normal corticomedullary organization. The immunostained *ts*1-GVT section (also see box in Fig. 1(A)) contains large, apparently uninfected (red, not yellow) CK8+ TECs within in an intact CMJ boundary (extending from lower left to upper right in the panel). In the same section, gp70-positive thymocytes surround the TECs. The next question, therefore, was: are the TECs and thymocytes dead in the thymi of *ts*1-only mice, and alive in the thymi of *ts*1-GVT mice?

3.2. Apoptosis is elevated in TECs and thymocytes of thymi ts1-infected mice, but not in infected mice treated with GVT

Caspase-3 is the executive enzyme that completes apoptotic cascades in most cell types. The presence of the activated (cleaved) form of caspase-3 is a specific indicator of apoptotic cell death in tissues, including the thymus [51]. In the *ts*1-only and *ts*1-GVT sections stained for CK8 and gp70 in Fig. 1(A) and (B), *ts*1-infected thymocytes and TECs are visible, but the images cannot tell us whether these cells are alive or dead. To find out, we compared levels of activated caspase-3 protein in thymocytes from these animals. The Western blot in Fig. 2(A) shows that *ts*1-only thymocytes contain elevated amounts of cleaved caspase-3, relative to uninfected thymocytes, while *ts*1-GVT thymocytes have somewhat less cleaved caspase-3, in relation to the *ts*1-only tissues. It should be noted that the relatively high levels of cleaved caspase-3 in uninfected thymocytes are normal, because most T cells generated in the thymus also undergo apoptosis there [45,46]. Thus, if the *ts*1-GVT thymus is functioning normally, cleaved caspase-3 levels should approach those of uninfected thymi, as they apparently do (Fig. 2(A)).

For an *in situ* look at caspase-3 in the thymi the three groups above, we stained 30 dpi thymic sections for gp70 or for cleaved caspase-3. The photomicrographs in Fig. 2(B) show that cells positive for gp70 are abundant in thymi from both *ts*1-only and *ts*1-GVT mice. However, while cleaved caspase-3-positive cells are abundant in the *ts*1-only thymus section, they are apparently absent in the *ts*1-GVT section (Fig. 3(C)).

3.3. Thymocyte numbers and weight are dramatically reduced in the ts1-only thymus, but not in thymi of infected mice treated with GVT

The loss or presence of cytokeratin-based corticomedullary organization in *ts*1-only thymi (Fig. 1), and the presence or absence of cleaved caspase-3 in these tissues (Fig. 2) are reliable but indirect markers of dysregulated (*ts*1-only) vs. apparently normal (*ts*1-GVT) T cell differentiation. To assess the state of T cell differentiation directly, we compared the total numbers of thymocytes, and thymic weights, for 30 dpi mice from the uninfected, GVT-only, *ts*1-only, and *ts*1-GVT treatment groups. The bar graphs in Fig. 3(A) show that statistically significant thymocyte loss is evident in 30 dpi mice from the *ts*1-only group, but not in the thymi of *ts*1-GVT mice ($p < 0.001$). Similarly, when we compared average thymus weights for the same mice, prior to isolation of their thymocytes,

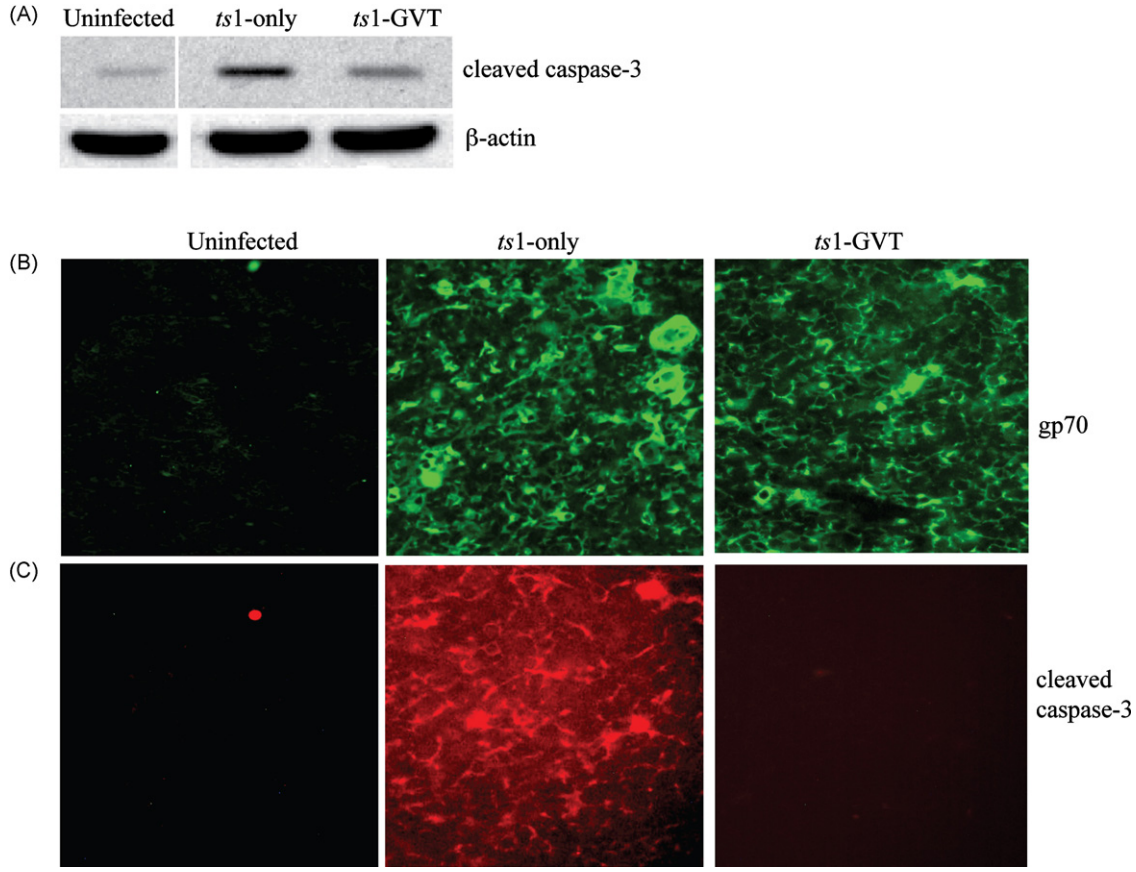

Fig. 2. Cells of the thymus die by apoptosis in *ts*1-only mouse thymi, but not if the thymi are from *ts*1-GVT animals. (A) Western blot of thymocyte lysates for comparison of their contents of activated caspase-3. The *ts*1-only thymocytes contain more of this enzyme than do uninfected thymocytes, while *ts*1-GVT thymocytes contain intermediate amounts. β-actin was used as a loading control. (B and C) Sections of thymi from mice of the three groups in (A), stained either for gp70 (green; to detect *ts*1 infection) and for cleaved caspase-3 (red). Both the *ts*1-only and the *ts*1-GVT sections have gp70-positive infected cells, but only the *ts*1-only section has cells that are positive for cleaved caspase-3. The sections from the *ts*1-GVT thymus are both from the thymic cortex; this may explain the unexpected absence of caspase-3-positive cells in the right lower panel in (C), given the presence of at least some cleaved caspase-3 in the thymic tissues of *ts*1-GVT mice. Original magnifications (A and B): all panels, 20×.

we observed, as expected, a significant loss of thymus weight in the 30 thymi of *ts*1-only mice (Fig. 3(B); $p < 0.001$). However, no thymic weight loss had occurred in 30 dpi infected mice if they had also been treated with GVT. A small but significant weight increase was evident in the *ts*1-only thymi, relative to the uninfected controls ($p < 0.05$).

3.4. ROS levels are reduced in thymi from GVT-treated mice

We next asked how GVT prevents thymocyte apoptosis in *ts*1-GVT mice, whose TECs and thymocytes are infected but alive at 30 dpi (Figs. 1–3). We had reported previously that oxidative stress is the trigger for apoptosis of *ts*1-infected astrocytes, and that oxidative stress also occurs in thymi of *ts*1-infected mice, but that GVT treatment prevents both astrocyte and thymocyte death *in situ* [29]. We therefore asked whether GVT treatment of mice actually affects the intracellular redox conditions in their thymocytes, using the fluorescent dye DCFDA to quantitate their contents of ROS [52]. The bar graphs in Fig. 4 show that thymocytes from GVT-treated mice do have significantly lower ROS contents than thymocytes from uninfected mice, whether the mice are infected or uninfected or not ($p < 0.001$, when compared either to uninfected or *ts*1-only thymocytes). These observations tell us two new and significant things: one, the ROS-lowering effects of GVT do not require concomitant infection with *ts*1 or other oxidant stressors, and, two, that GVT treatment somehow sets up conditions in which a steady-state redox "tone" is established and maintained in thymocytes of infected treated animals, thus presumably affecting all intracellular parameters impacted by ROS levels in the cells. These results link GVT protection of the thymus to events that reduce ROS levels in thymocytes, and they suggest that GVT protects thymocytes by setting up low-ROS conditions that allow *ts*1 infection of thymocytes, but prevent the cytopathology and apoptosis that otherwise would kill the infected cells. How might these low-ROS conditions be established in the thymocytes by GVT?

3.5. Nrf2 upregulation and stabilization in TECs of thymi from GVT-treated, infected mice

To determine how GVT might cause lowering of redox setpoints in thymocytes, we took into account results from our earlier published studies using cultured astrocytic cells [29,37,38]. When these cells were infected in culture with *ts*1, about 50% of the cells died, but 50% remained alive, and these could be passaged over a long period of time [38]. Notably, the astrocytes that survived were different from those that died, with respect to (a) their maintenance of low steady-state ROS levels, and (b) their high levels of Nrf2 [38]. These results suggested that the high Nrf2 levels in *ts*1-infected astrocytes were causally linked to their low ROS.

Many cell types, including astrocytes, maintain ambient levels of the Nrf2 protein, which is a transcription factor that coordinately upregulates many genes that participate in Phase 2 antioxidant defenses. In non-stressed cells, Nrf2 is held in an inactive state as part of a complex with the Keap-1 molecule. As long as steady-state conditions prevail, the complexed Nrf2 is cyclically ubiquitinated, released to the proteasomes for degradation, and replaced by newly

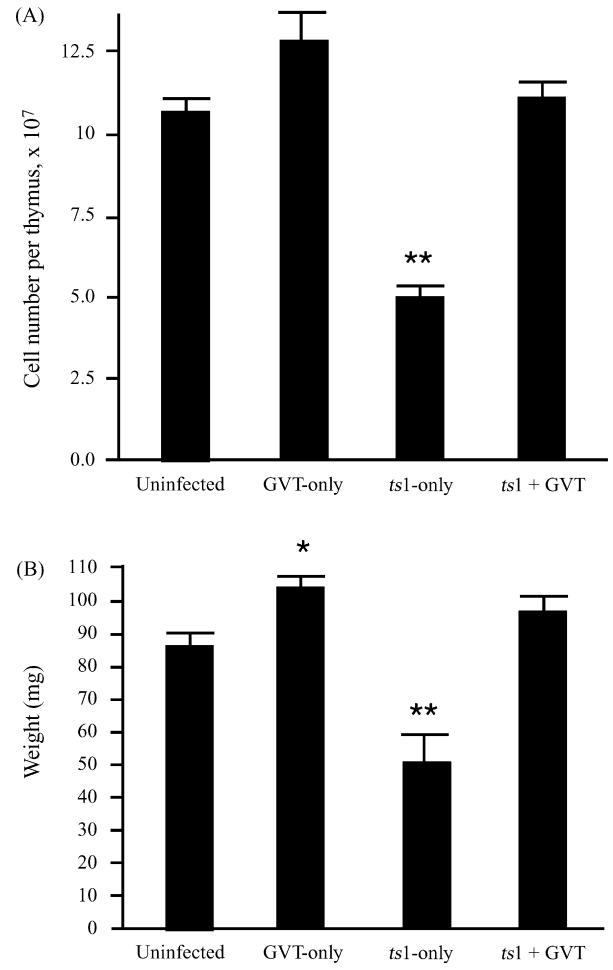

Fig. 3. Total numbers of thymocytes and average thymic weights in 30 dpi thymi from uninfected, GVT-only, *ts*1-only, and *ts*1-GVT mice. (A) The bar graphs show the means ± standard deviations for total numbers of thymocytes for five mice from each group. $^{**}p < 0.001$ for *ts*1-only mice vs. each of the three other groups. (B) The bar graphs show the average weights for thymi of the four groups in (A). $^{**}p < 0.001$ for *ts*1-only mice vs. each of the three other groups; $^{*}p < 0.05$ when compared to uninfected thymi.

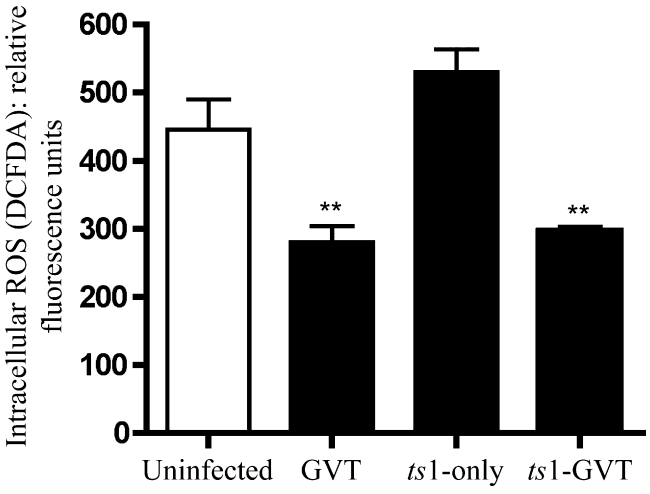

Fig. 4. Thymocyte ROS contents are reduced in mice treated with GVT, whether or not they are infected. The bar graphs show the average of relative numbers of fluorescence units of DCFDA in lysates of thymocytes from uninfected, GVT-only, *ts*1-only and *ts*1-GVT mice, represented as the mean ± standard deviations for values for three mice of each group. $^{**}p < 0.001$ for thymocytes of GVT-treated mice (infected or not) vs. thymocytes from uninfected or *ts*1-only mice.

translated Nrf2 [53–55]. When oxidant stress conditions occur, however, redox-sensitive sites on the Keap-1 protein allow it to release Nrf2, which is then phosphorylated and transported to the nucleus. In the nucleus, Nrf2 activates genes that have ARE sequences in their promoters (reviewed in [54]).

When ROS levels in the cells are returned to normal, it has been assumed that the activated Nrf2 that is left is ubiquitinated and degraded. However, our results for astrocytes [38], and recent work by other laboratories, have shown that Nrf2 levels can be stabilized in the cytoplasm and nucleus under certain kinds of oxidant stress conditions [56], or by drugs that inhibit Nrf2 degradation in proteasomes [57,58]. Agents that stabilize Nrf2 levels in cells have been identified as having anti-inflammatory effects, most likely due to the continued or amplified antioxidant defenses that might be available to cells as a consequence [57]. We therefore asked whether Nrf2 upregulation and stabilization occurs in thymocytes of *ts*1-GVT mice.

The results of these experiments are in Fig. 5. Surprisingly and against our expectations, our first Western blots for Nrf2, performed with isolated thymocytes, show that Nrf2 levels of *ts*1-only and *ts*1-GVT mice are only slightly upregulated over levels in uninfected thymocytes (Fig. 5(A)). This result was also obtained in an earlier publication from this laboratory [29]. To find out whether Nrf2 upregulation instead occurs in other cells in the thymus, we performed a second Nrf2 Western blot, this time using whole thymus tissue. The results in this Western blot in Fig. 5(B) indicate that whole thymus tissues from *ts*1-only and *ts*1-GVT mice have a two-fold increase in amounts of Nrf2, over those of uninfected cells. We conclude that thymocytes of *ts*l-only or *ts*1-GVT mice do not change their Nrf2 levels, but that other cells in the thymus do. This result poses a different scenario from the one we had constructed when designing this experiment, in which thymocytes of *ts*1-GVT mice protect themselves by upregulating their Nrf2 levels, as do astrocytes that survive *ts*1 infection [38]. If Nrf2 plays a role in lowering *ts*1-GVT thymocyte ROS levels, and if low-ROS conditions are responsible for the survival of these cells, then Nrf2 upregulation and stabilization may occur in cells that support thymocyte redox homeostasis, rather than in thymocytes themselves.

There are many non-thymocyte cell types in the normal thymus, including dendritic cells, macrophages, and TECs [59]. Others have shown that dendritic cells control T cell activation events via the T cell receptor, by regulating the redox environment of antigen presentation and recognition [58]. In thymi of *ts*1-GVT mice, the cells most likely to play a supporting role of this type would be the TECs. In addition to hosting thymocyte differentiation, TECs may provide metabolic and redox support to thymocytes via Nrf2 stabilization and release of thiol redox antioxidants to thymocytes, just as astrocytes do for neurons in the CNS under oxidant stress [60].

Our early published work has shown that thymocytes of FVB/N mice can be cultured and infected by *ts*1 in vitro, but only if IL-2 and IL-7 (produced by thymocytes and TECs, respectively) are added to the culturing medium, and only if the culturing wells contain thymic remnants [61]. More recent studies with HIV-1 have produced similar results, in showing that TECs must be present for infection of cultured thymocytes [62]. For *ts*1 and HIV-1 infection of cultured thymocytes, therefore, TECs may be required to make virus available for thymocyte infection, or to provide metabolic or redox support for infected thymocytes. For the same reasons, GVT protection of thymocytes may require the presence of TECs that can upregulate and stabilize their Nrf2. To determine whether this might be the case, we first prepared frozen sections of uninfected *ts*1-only vs. *ts*1-GVT thymi, and doubly stained them with gp70 and Nrf2. The photomicrographs in Fig. 5(C) show that the *ts*1-only thymic section contains many large, infected gp70-positive cells, all of which also contain Nrf2 (no red cells are present, indicating that all Nrf2-positive cells are also infected). By contrast, the

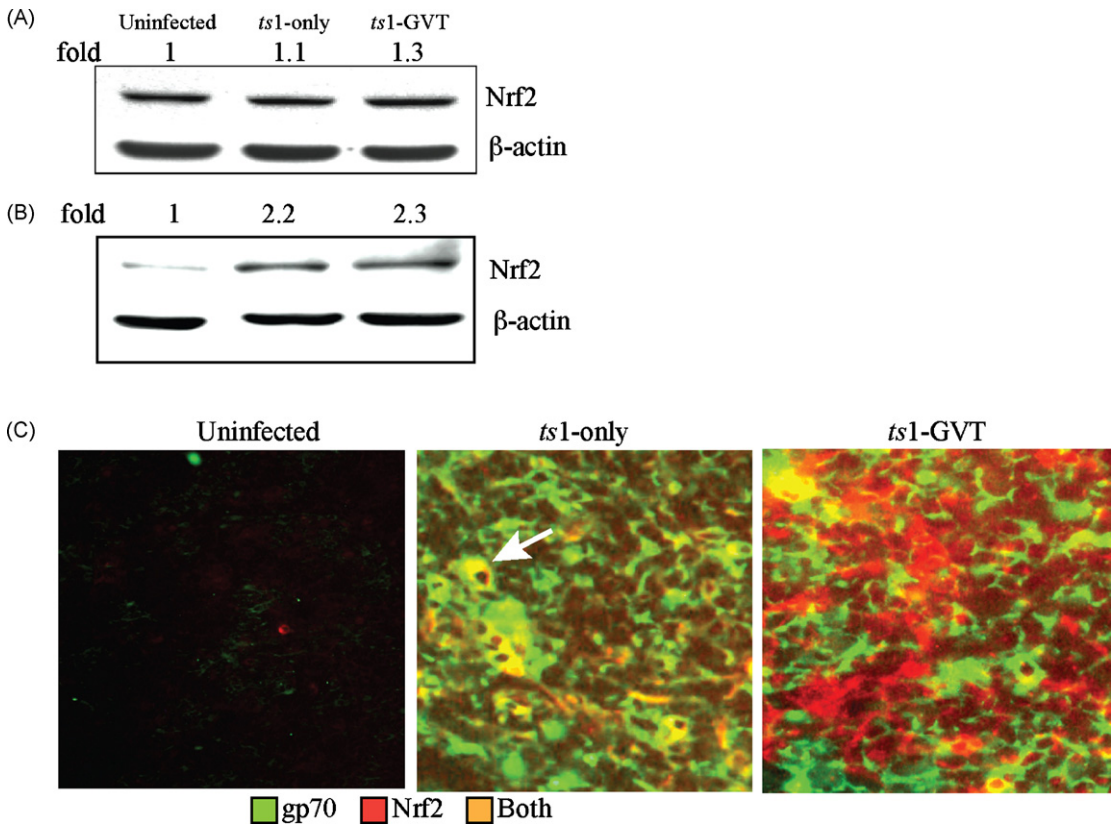

Fig. 5. Levels of the transcription factor Nrf2 are not significantly elevated in *ts*1-only or *ts*1-GVT mouse thymocytes at 30 dpi, but are in whole thymic tissues, where the protein is concentrated in non-thymocytic cells. (A) Western blot of thymocyte lysates compared for their amounts of Nrf2. Fold difference calculations disclosed no significant differences were evident among uninfected, *ts*1-only and *ts*1-GVT thymocytes. (B) Western blot of whole thymic tissue lysates from animals of the same three treatment groups. Amounts of Nrf2 in the *ts*1-only and *ts*1-GVT tissues were at least twice those in uninfected tissues, indicating that some cell type(s) in the thymus do upregulate their Nrf2 levels after *ts*1 infection in *ts*1-only and *ts*1-GVT thymi. (C) Sections of thymi from mice of the three different treatment groups in (A) and (B), doubly immunostained for gp70 (green, for infection) and for Nrf2 (red). In the *ts*1-only section, not all gp70-positive infected cells are yellow (co-stained for both markers), but all Nrf2-positive cells are. By contrast, sections of thymi from *ts*1-GVT mice contain both gp70-positive (infected cells) and Nrf2-positive cells, but the cells stained by the two antibodies are largely either green or red, but not yellow, indicating that they express either gp70 or Nrf2, but not both.

thymic section from the *ts*1-GVTmouse shows many gp70-positive infected cells (green; without Nrf2), but also has large numbers of red cellular profiles (Nrf2-positive only) that are not thymocytes.

To determine whether these Nrf2-positive cells are TECs, we stained one *ts*1-only and one *ts*1-GVT section for Nrf2 and CK8. Fig. 6(A) shows that all of the Nrf2-positive cells in *ts*1-only section are CK8-positive cortical epithelial cells, but that these cells lack organization and appear to be dying or dead. In the *ts*1-GVT section, however (Fig. 6(B)), the epithelial cells are intact, and all of the cells are positive for Nrf2 and CK8 (yellow). We conclude that TECs upregulate and stabilize their Nrf2 in *ts*1-GVT thymi, and that this TEC loading with Nrf2 may maintain low-ROS conditions in their thymocytes, most likely by providing the thymocytes with cysteine substrates or GSH.

3.6. *gPr80^{env} is processed normally in thymocytes of infected, GVT-treated mice*

One possible consequence of low-ROS conditions in thymocytes of *ts*1-GVT mice might be the normal processing of gPr80^{env} to gp70 and PrP15E in infected thymocytes. As noted above, we have established that *ts*1-infected astrocytes and thymocytes die as a consequence of accumulation of the mutant *ts*1 preprotein gPr80^{env} in the ER. Accumulation of gPr80^{env} triggers the UPR, which in turn elicits ER stress and calcium loading into mitochondria, causing mitochondrial and oxidant stress-induced apoptosis [29–38]. In normal cells, the local redox environment in the ER is controlled to provide reducing conditions necessary for formation of disulfide bonds, and to promote or inhibit hydrogen bonding during the translation of proteins with complex folding requirements [63]. We therefore wondered whether the low-ROS conditions in *ts*1-GVT thymocytes might allow normal folding and processing of the *ts*1 mutant gPr80^{env}. This would protect them from the apoptotic cascades that are activated in thymocytes of *ts*1-only mice.

To determine whether this occurs, we used Western blotting with anti-gp70 to compare amounts of gPr80^{env} (uncleaved) to gp70 (cleaved) envelope protein in thymocytes of *ts*1-only vs. *ts*1-GVT mice. The results in Fig. 7 show that *ts*1-only infected tissues contain both aggregated gPr80^{env} at 80 kDa, and processed gp70, at 70 kDa. This is a typical Western blotting result from *ts*1-infected astrocytes and thymocytes, whose processing of gPr80^{env} is inefficient [26–29]. By contrast, all of the gp70-immunoreactive protein is in the 70 kDa band from thymocytes of *ts*1-GVT mice, indicating that the gPr80^{env} is being processed normally in these cells.

4. Discussion

Like *ts*1, other cytopathic retroviruses, including HIV-1, SIV and FIV, cause damage to thymic cytoarchitecture and loss of thymocytes in their respective host species, making the thymus unable to supply naïve T cells for protective immune responses to viral variants as they appear during the disease course [8–10,13,63–65]. HAART therapies, like those currently in use for treatment of HIV-AIDS, may not restore thymopoiesis even assuming that normal Tprogenitor cells are produced and sent to the thymus from the bone marrow in these patients [66]. This means that naïve T cell

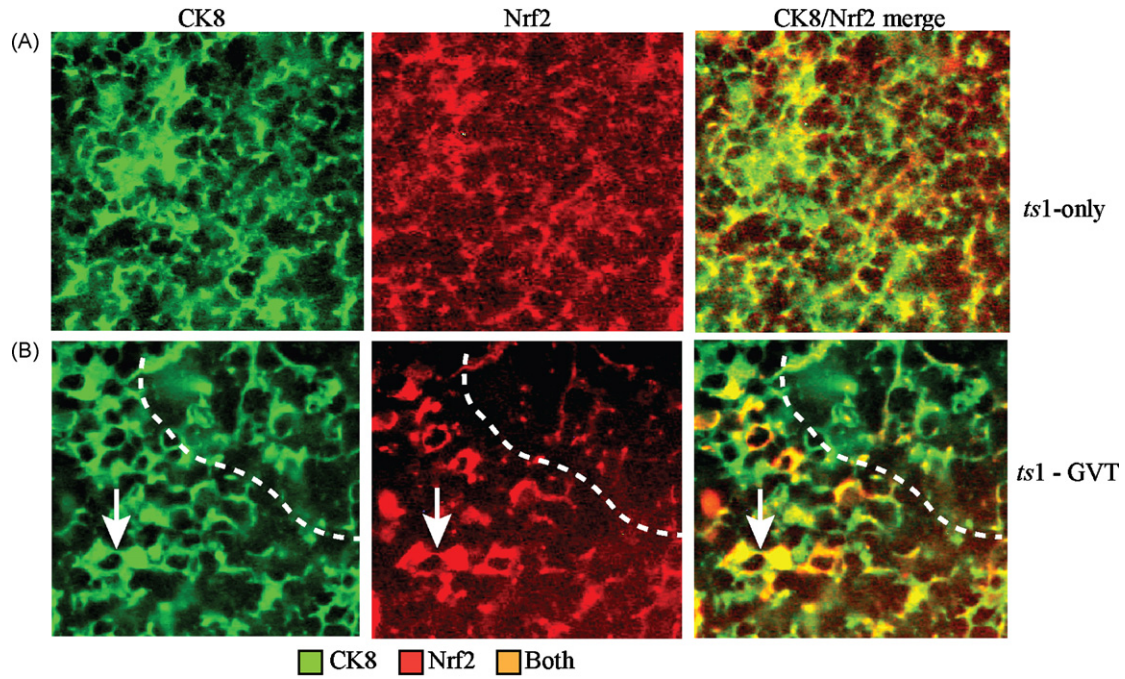

Fig. 6. The Nrf2-positive cells in *ts*1-only and *ts*1-GVT thymi are CK8-positive TECs. The thymic section in (A) was doubly stained with anti-gp70 (green) to detect infection, and with anti-Nrf2 (red). The merged panel from these images, at the right, shows a generally disorganized tissue containing TECs and thymocytes, without a clear pattern of co-staining for the two. By contrast, the thymic section in (B), which was stained in the same way, contains a clear Nrf2-defined area, with CK8-positive cells on the left and right side (line in all panels), and Nrf2-positive cells on the left side. The arrows in all panels in (B) point to a CK8-positive, Nrf2-positive cortical TEC.

exhaustion, thought to be one cause of HIV-1 immunosuppression [9–11] might still occur under HAART treatment. For the same reasons, bone marrow or hematopoietic stem cell transplantation, once considered as potential treatments for T cell exhaustion in HIV-AIDS [66–68], may not repopulate the thymus either, unless there is a functioning and non-toxic (e.g., low-ROS) microenvironment there in which the stem cells can differentiate to become T cells.

The results of this study may address some of these problems, although they come from studies of what happens to the mouse thymus infected by only one type of T cell-tropic retrovirus. The work reported here confirms that TEC and thymocyte loss following *ts*1 retroviral infection are not the results of infection *per se*, but rather are the result of oxidative stress leading to apoptosis of thymocytes. If oxidative stress also occurs in the HIV-AIDS thymus and thymocytes, and if GVT can reduce or eliminate it even as the cells remain infected, then repopulation of the thymus might be possible in these patients, either by autologous bone marrow T cell progenitors or by transplanted bone marrow stem cells [66–68].

GVT is an antioxidant compound that has anti-inflammatory and anti-apoptotic properties in many animal and human diseases [29,69–73]. GVT is also a non-toxic drug in mice [29] and humans [69–73]. When we started these studies, we already knew that GVT protects the thymi of *ts*1-infected mice, both at the gross level (by maintaining normal thymus weight) and the cellular level (by preventing oxidative stress in thymic cells) [29]. In *ts*1 infection, the thymus appears to be a "staging area" from which infectious virus is disseminated to other tissues, including the CNS; in fact, a thymus must be present if CNS and then systemic infection are to occur [74]. The simplest way to interpret the systemic protective effect of GVT in *ts*1 infection, then, would start with the thymus. The survival and apparent homeostasis of its TEC and thymocyte cell compartments, under GVT treatment, could be the basis of what becomes either a fatal disease or a harmless infection in other tissues as well (including the intestine [97]). In the *ts*1-GVT thymus, we have shown here (1) that the TECs maintain normal characteristics in *ts*1-GVT mice; (2) that thymocytes of *ts*1-GVT mice survive despite continued infection; (3) that the thymocytes have lower than normal ROS levels; (4) that TEC Nrf2 levels are upregulated and stabilized; and (5) that these thymocytes do not contain accumulated $gPr80^{env}$. If the first of these is causally linked in series to the last, then the prosurvival effects of low ROS conditions, caused by GVT, could either be direct (via GVT alone) or indirect, via GVT upregulation and stabilization of Nrf2. A diagram showing these possible pathways is provided in Fig. 8.

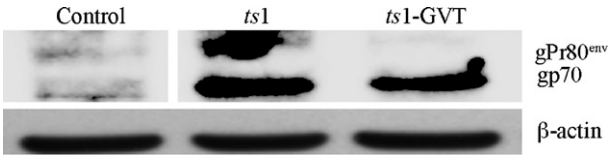

Fig. 7. Western blot of 30 dpi thymic tissues from uninfected, *ts*1-only and *ts*1-GVT mice, probed for gp70. The antibody identifies epitopes present in both the band present at 80 kDa, which is $gPr80^{env}$ (the viral preprotein), and in the band at the 70 kDa position (gp70). This blot shows that $gPr80^{env}$ accumulation occurred in this *ts*1-only thymus, but not in the thymic tissues of the *ts*1-GVT mouse whose tissues were used for this blot. Some *ts*1-GVT thymi contain $gPr80^{env}$ at 30 dpi, but in significantly smaller amounts than those seen for thymi of *ts*1-only mice, and with a correspondingly larger gp70 band, than those seen for *ts*1-only thymi (not shown).

Given that other retrovirus infections involve oxidative stress (including HIV-1 and SIV; see below), it is tempting to speculate that GVT treatment could prevent thymocyte loss and maintain normal thymic cytoarchitecture in all cytopathic retroviral diseases. As noted above, we believe that the *ts*1-infected mouse is a model for HIV-AIDS, despite differences between the two viruses and the diseases they cause [16–23]. Matching characteristics between the *ts*1-infected mouse and the HIV-infected human have been identified in published papers from our laboratory and from others [16,19–21]. The *ts*1 virus selectively infects and kills CD4+ peripheral T cells [18,19,22,23] and CD4+ thymocytes (V.L. Scofield et al., in preparation).

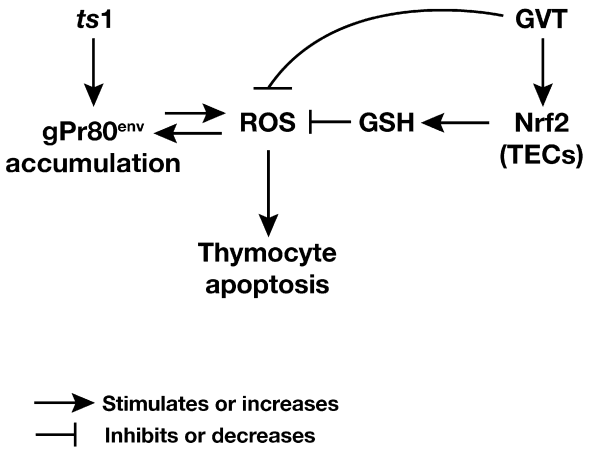

Fig. 8. Diagram showing possible mechanisms for protection of 30 dpi *ts*1-infected mouse thymi and their thymocytes by GVT. The arrows point to processes initiated or promoted by *ts*1 infection or GVT treatment, and the T-bars identify GVT inhibition or termination of processes initiated by *ts*1 infection in T cells. In the *ts*1-only mouse, both TECs and thymocytes are damaged. The result is the disappearance of epithelial cell gradients, loss of thymocytes, and thymic atrophy. In the *ts*1-GVT mouse, the epithelial cells and thymocyte compartments appear normal, although the TECs accumulate and stabilize their Nrf2, and the thymocytes have lower-than-normal ROS levels. The thymocytes and TECs survive infection, and gPr80^{env} does not accumulate in infected thymocytes. As for the intestine [97], our data suggest that this protection could occur either in two ways: via direct antioxidant activity by GVT, or lowering of thymocyte intracellular redox setpoints by gluthione (GSH) or by GSH precursors, both produced and provided to the thymocytes by TECs as a consequence of their upregulation of Nrf2.

Although it might be argued that the abnormal protein accumulation and oxidative stress that kill *ts*1-infected thymocytes do not participate in T cell loss in HIV-1 infection, we would respond by pointing out that this question has not been experimentally tested in a direct way. Given that the mechanisms leading to thymocyte and T cell death in HIV-AIDS are still not known [2,10], we would suggest that this issue now be the object of concentrated investigation in HIV-AIDS. Dozens of studies over the past decades now suggest that abnormal viral protein accumulation [75–78] and/or oxidative stress [79–93] occur in loss of T cells in HIV-AIDS. Recent work has shown that folding of nascent membrane proteins in the ER of healthy cells depends upon a carefully controlled intracellular redox environment [63,78,94]. In cells whose ROS levels have risen due to oxidant challenge, misfolding theoretically is a possibility for all membrane proteins in the cell. In light of this, it is interesting to note that the HIV-1 membrane preprotein gp160 has particularly strict requirements for sequential and complex folding events [78], and that these make it especially likely to misfold and aggregate when ROS levels increase in infected cells. Since *ts*1 gPr80^{env} misfolds in thymocytes whose ROS levels are near normal or only slightly elevated (Figs. 4 and 7), the lowering of ROS caused by GVT treatment in thymocytes of *ts*1-GVT mice may promote normal folding of gpr80^{env}. If this occurs, it may be why TECs and thymocytes in *ts*1-GVT mice survive infection (Fig. 8). We hope that the findings reported here will re-awaken the possibility that abnormal protein accumulation, followed by oxidative stress, might lead to the killing of thymocytes and T cells in HIV-AIDS and in other retroviral syndromes that target these cells. If so, then GVT and other antioxidant compounds may allow maintenance or restoration of a normal thymic microenvironment in HIV-AIDS patients, allowing the differentiation of autologous bone marrow T cell progenitors, or of T cell progenitors from bone marrow or stem cell allotransplants [95,96]. As an antioxidant, GVT may prove to have wider therapeutic utility as a non-toxic anti-inflammatory drug that exploits natural antioxidant mechanisms (e.g., Nrf2) to prevent tissue damage after oxidant injury.

Acknowledgements

This paper is dedicated by the first author to the memory of Professor John J. Marchalonis (1941–2007). We thank the late Dr. David Klug for important discussions, and we acknowledge indispensable help and advice from Carla Carter and Dr. Ellen Richie. We also thank Shawna Johnson and Rebecca Deen for assistance in preparing the manuscripts, Kent Claypool for providing invaluable help with flow cytometry analysis, and Nancy Otto and Jimi Lynn Brandon, of the Science Park Histology Core, for preparing excellent frozen sections and for advising us regarding immunohistochemical analysis. This work was supported by NIH grants NS43984 and MH71583 (P.K.Y.), by a Career Re-entry supplement to MH71583 for V.L.S., and by NIH grant MH077470 (V.L.S.). Other support was provided by NIEHS Center Grant ES07784 and Core Grant CA16672, both to the M.D. Anderson Cancer Center, Science Park-Research Division, Smithville, TX, by the Dr. Christian Abee of the Michale E. Keeling Center for Comparative Medicine and Research, The University of Texas M.D. Anderson Cancer Center, Bastrop, TX, and by the Longevity Foundation of Austin.

References

[1] Barth CF, Ewert DL, Olson WC, Humphries EH. Reticuloendotheliosis virus REVT(REV-A)-induced neoplasia: development of tumors within the T-lymphoid and myeloid lineages. J Virol 1990;64:6054–62.
[2] O'Neill HC. The diversity of retroviral diseases of the immune system. Immunol Cell Biol 1992;70(Pt 3):193–9.
[3] Tompkins MB, Tompkins WA. Lentivirus-induced immune dysregulation. Vet Immunol Immunopathol 2008;123:45–55.
[4] Veazey RS, Tham IC, Mansfield KG, DeMaria M, Forand AE, Shvetz DE, et al. Identifying the target cell in primary simian immunodeficiency virus (SIV) infection: highly activated memory CD4$^+$ T cells are rapidly eliminated in early SIV infection in vivo. J Virol 2000;74:57–64.
[5] Panda BR, Kingsman SM, Kingsman AJ. Mutational analysis of the putative receptor binding domain of Moloney murine leukemia virus glycoprotein gp70. Virology 2000;273:90–100.
[6] Rasko JE, Battini JL, Gottschalk RJ, Mazo I, Miller AD. The RD$_{114}$/simian type D retrovirus receptor is a neutral amino acid transporter. Proc Natl Acad Sci USA 1999;96:2129–34.
[7] Reggeti F, Ackerley C, Bienzle D. CD134 and CXCR4 expression corresponds to feline immunodeficiency virus infection of lymphocytes, macrophages and dendritic cells. J Gen Virol 2008;89:277–87.
[8] Bonzon C, Fan H. Moloney murine leukemia virus-induced preleukemic thymic atrophy and enhanced thymocyte apoptosis correlate with disease pathogenicity. J Virol 1999;73:2434–41.
[9] El-Far M, Halwani R, Said E, Trautmann L, Doroudchi M, Janbazian L, et al. T-cell exhaustion in HIV infection. Curr HIV/AIDS Rep 2008;5:13–9.
[10] Ho Tsong Fang R, Colantonio AD, Uittenbogaart CH. The role of the thymus in HIV infection: a 10 year perspective. AIDS 2008;22:171–84.
[11] Marmor MD, Benatar T, Ratcliffe MJ. Retroviral transformation in vitro of chicken T cells expressing either/or γ/δ T cell receptors by reticuloendotheliosis virus strain T. J Exp Med 1993;177:647–56.
[12] Mexas AM, Fogle JE, Tompkins WA, Tompkins MB. CD4$^+$ CD25$^+$ regulatory T cells are infected and activated during acute FIV infection. Vet Immunol Immunopathol 2008.
[13] Prukova D, Vernerova Z, Pilcik T, Stepanets V, Indrova M, Geryk J, et al. Differences in pathogenicity among strains of the same or different avian leukosis virus subgroups. Avian Pathol 2007;36:15–27.
[14] Schindler M, Schmokel J, Specht A, Li H, Munch J, Khalid M, et al. Inefficient Nefmediated downmodulation of CD3 and MHC-I correlates with loss of CD$_4^+$ T cells in natural SIV infection. PLoS Pathog 2008;4:e1000107.
[15] Wong PK, McCarter JA. Genetic studies of temperature-sensitive mutants of Moloneymurine leukemia virus. Virology 1973;53:319–26.
[16] Wong PK, Szurek PF, Floyd E, Saha K, Brooks BR. Alteration from T- to B-cell tropism reduces thymic atrophy and cytocidal effects in thymocytes but not neurovirulence induced by *ts*1, a mutant of Moloney murine leukemia virus TB. Proc Natl Acad Sci USA 1991;88:8991–5.
[17] Chakraborty J, Clark S, Okonta H, Duggan J. A small animal model for mother-to-fetus transmission of *ts*1, a murine retrovirus. Viral Immunol 2003;16:191–201.
[18] Clark S, Duggan J, Chakraborty J. *ts*1 and LP-BM5: a comparison of two murine retrovirus models for HIV. Viral Immunol 2001;14:95–109.
[19] Saha K, Wong PK. *ts*1, a temperature-sensitive mutant of Moloney murine leukemia virus TB, can infect both CD4$^+$ and CD8+ T cells but requires CD4$^+$ T cells in order to cause paralysis and immunodeficiency. J Virol 1992;66:2639–46.
[20] Stoica G, Floyd E, Illanes O, Wong PK. Temporal lymphoreticular changes caused by *ts*1, a paralytogenic mutant of Moloney murine leukemia virus TB. Lab Invest 1992;66:427–36.

[21] Wong PKY, Lynn WS, Lin YC, Choe W, Yuen PH. *ts*1-MoMuLV: a murine model of neuroimmunodegeneration. Neuroimmunodegeneration 1998:75–93.
[22] Saha K, Wong PK. T, not B, lymphocytes are required for immunodeficiency and paralysis induced by *ts*1, a mutant of Moloney murine leukemia virus-TB. Virology 1991;183:815–20.
[23] Saha K, Yuen PH, Wong PK. Murine retrovirus-induced depletion of T cells is mediated through activation-induced death by apoptosis. J Virol 1994;68:2735–40.
[24] Wong PK, Prasad G, Hansen J, Yuen PH. *ts*1, a mutant of Moloney murine leukemia virus-TB, causes both immunodeficiency and neurologic disorders in BALB/c mice. Virology 1989;170:450–9.
[25] Gonzales-Scarano F, Nathanson N, Wong PKY. Retroviruses and the nervous system. In: Levy JA, editor. The retroviridae. New York, NY: Plenum Press; 1995. p. 409–90.
[26] Szurek PF, Yuen PH, Ball JK, Wong PKY. A Val-25-to-Ile substitution in the envelope precursor protein, gPr80^{env}, is responsible for the temperature sensitivity, inefficient processing of gPr80^{env}, and neurovirulence of *ts*1, a mutant of Moloney murine leukemia virus TB. J Virol 1990;64:467–75.
[27] Kamps CA, Lin Y-C, Wong PKY. Oligomerization and transport of the envelope protein of Moloney murine leukemia virus-TB and of *ts*1, a neurovirulent temperature-sensitive mutant of MoMuLV-TB. Virology 1991;184:687–94.
[28] Yu Y, Wong PK. Studies on compartmentation and turnover of murine retrovirus envelope proteins. Virology 1992;188:477–85.
[29] Jiang Y, Scofield VL, Yan M, Qiang W, Liu N, Reid AJ, et al. Retrovirus-induced oxidative stress with neuroimmunodegeneration is suppressed by antioxidant treatment with a refined monosodium α-luminol (Galavit). J Virol 2006;80:4557–69.
[30] Kim HT, Qiang W, Wong PK, Stoica G. Enhanced proteolysis of IκBα and IκBβ proteins in astrocytes by Moloney murine leukemia virus (MoMuLV)-*ts*1 infection: a potential mechanism of NF-κB activation. J Neurovirol 2001;7:466–75.
[31] Kim HT, Tasca S, Qiang W, Wong PK, Stoica G. Induction of p53 accumulation by Moloney murine leukemia virus-*ts*1 infection in astrocytes via activation of extracellular signal-regulated kinases 1/2. Lab Invest 2002;82:693–702.
[32] Kim HT, Waters K, Stoica G, Qiang W, Liu N, Scofield VL, et al. Activation of endoplasmic reticulum stress signaling pathway is associated with neuronal degeneration in MoMuLV-*ts*1-induced spongiform encephalomyelopathy. Lab Invest 2004;84:816–27.
[33] Kim HT, Qiang W, Liu N, Scofield VL, Wong PK, Stoica G. Up-regulation of astrocyte cyclooxygenase-2, CCAAT/enhancer-binding protein-homology protein, glucose-related protein 78, eukaryotic initiation factor 2α, and c-Jun N-terminal kinase by a neurovirulent murine retrovirus. J Neurovirol 2005;11:166–79.
[34] Liu N, Qiang W, Kuang X, Thuillier P, Lynn WS, Wong PK. The peroxisome proliferator phenylbutyric acid (PBA) protects astrocytes from *ts*1 MoMuLV-induced oxidative cell death. J Neurovirol 2002;8:318–25.
[35] Liu N, Kuang X, Kim HT, Stoica G, Qiang W, Scofield VL, et al. Possible involvement of both endoplasmic reticulum- and mitochondria-dependent pathways in MoMuLV-*ts*1- induced apoptosis in astrocytes. J Neurovirol 2004;10:189–98.
[36] Liu N, Scofield VL, Qiang W, Yan M, Kuang X, Wong PK. Interaction between endoplasmic reticulum stress and caspase 8 activation in retrovirus MoMuLV-*ts*1-infected astrocytes. Virology 2006;348:398–405.
[37] Qiang W, Cahill JM, Liu J, Kuang X, Liu N, Scofield VL, et al. Activation of transcription factor Nrf-2 and its downstream targets in response to Moloney murine leukemia virus *ts*1-induced thiol depletion and oxidative stress in astrocytes. J Virol 2004;78:11926–38.
[38] Qiang W, Kuang X, Liu J, Liu N, Scofield V, Stoica G, et al. Astrocytes survive chronic infection and cytopathic effects of the *ts*1 mutant of the retrovirus Moloney murine leukemia virus by upregulation of antioxidant defenses. J Virol 2006;80:3273–84.
[39] Lungu GF, Stoica G, Wong PKY. Down-regulation of Jab1, HIF-1a, and VEGF by Moloney murine leukemia virus-*ts*1 infection: a possible cause of neurodegeneration. J Neurovirol 2008;14:239–51.
[40] Suzuki YJ, Forman HJ, Sevanian A. Oxidants as stimulators of signal transduction. Free Radic Biol Med 1997;22:269–85.
[41] Day RM, Suzuki YJ. Cell proliferation, reactive oxygen and cellular glutathione. Dose Response 2005;3:425–42.
[42] Winterbourn CC, Hampton MB. Thiol chemistry and specificity in redox signaling. Free Radic Biol Med 2008;45:549–61.
[43] Moi P, Chan K, Asunis I, Cao A, Kan YW. Isolation of NF-E2-related factor 2 (Nrf2), a NF-E2-like basic leucine zipper transcriptional activator that binds to the tandem NFE2/AP1 repeat of the β-globin locus control region. Proc Natl Acad Sci USA 1994;91:9926–30.
[44] Lau A, Villeneuve NF, Sun Z, Wong PK, Zhang DD. Dual roles of Nrf2 in cancer. Pharmacol Res 2008.
[45] Boehm T. Thymus development and function. Curr Opin Immunol 2008;20:178–84.
[46] Rodewald HR. Thymus organogenesis. Annu Rev Immunol 2008;26:355–88.
[47] Li B, Gladden AD, Altfeld M, Kaldor JM, Cooper DA, Kelleher AD, et al. Rapid reversion of sequence polymorphisms dominates early human immunodeficiency virus type 1 evolution. J Virol 2007;81:193–201.
[48] Zlotoff DA, Schwarz BA, Bhandoola A. The long road to the thymus: the generation, mobilization, and circulation of T-cell progenitors in mouse and man. Semin Immunopathol 2008 [Epub ahead of print].
[49] Klug DB, Carter C, Crouch E, Roop D, Conti CJ, Richie ER. Interdependence of cortical thymic epithelial cell differentiation and T-lineage commitment. Proc Natl Acad Sci USA 1998;95:11822–7.
[50] Klug DB, Crouch E, Carter C, Coghlan L, Conti CJ, Richie ER. Transgenic expression of cyclin D1 in thymic epithelial precursors promotes epithelial and T cell development. J Immunol 2000;164:1881–8.
[51] Minter LM, Osborne BA. Cell death in the thymus—it' s all a matter of contacts. Semin Immunol 2003;15:135–44.
[52] LeBel CP, Ali SF, McKee M, Bondy SC. Organometal-induced increases in oxygen reactive species: the potential of 2′,7′-dichlorofluorescein diacetate as an index of neurotoxic damage. Toxicol Appl Pharmacol 1990;104:17–24.
[53] Alam J, Killeen E, Gong P, Naquin R, Hu B, Stewart D, et al. Heme activates the heme oxygenase-1 gene in renal epithelial cells by stabilizing Nrf2. Am J Physiol Renal Physiol 2003;284:F743–752.
[54] Nguyen T, Yang CS, Pickett CB. The pathways and molecular mechanisms regulating Nrf2 activation in response to chemical stress. Free Radic Biol Med 2004;37:433–41.
[55] Zhang DD, Hannink M. Distinct cysteine residues in Keap1 are required for Keap1-dependent ubiquitination of Nrf2 and for stabilization of Nrf2 by chemopreventive agents and oxidative stress. Mol Cell Biol 2003;23:8137–51.
[56] Purdom-Dickinson SE, Sheveleva EV, Sun H, Chen QM. Translational control of Nrf2 protein in activation of antioxidant response by oxidants. Mol Pharmacol 2007;72:1074–81.
[57] Gharavi N, Haggarty S, El-Kadi AO. Chemoprotective and carcinogenic effects of tertbutylhydroquinone and its metabolites. Curr Drug Metab 2007;8:1–7.
[58] Kim HJ, Barajas B, Wang M, Nel AE. Nrf2 activation by sulforaphane restores the agerelated decrease of T_H1 immunity: role of dendritic cells. J Allergy Clin Immunol 2008;121(1255–1261):e1257.
[59] Su DM, Manley NR. Stage-specific changes in fetal thymocyte proliferation during the $CD4^-8^-$ to $CD4^+8^+$ transition in wild type, *Rag1*$^{-/-}$, and *Hoxa3,Pax1* mutant mice. BMC Immunol 2002;3:12.
[60] Vargas MR, Pehar M, Cassina P, Beckman JS, Barbeito L. Increased glutathione biosynthesis by Nrf2 activation in astrocytes prevents p75^{NTR}-dependent motor neuron apoptosis. J Neurochem 2006;97:687–96.
[61] Wong PKY, Saha K, Lin Y-C, Lynn WS, Yuen PH. Long term cultivation and productive infection of primary thymocyte cultures by a thymocytopathic murine retrovirus. Virology 1996;215:203–6.
[62] Rothe M, Chene L, Nugeyre MT, Braun J, Barre-Sinoussi F, Israel N. Contact with thymic epithelial cells as a prerequisite for cytokine-enhanced human immunodeficiency virus type 1 replication in thymocytes. J Virol 1998;72:5852–61.
[63] Ushioda R, Hoseki J, Araki K, Jansen G, Thomas DY, Nagata K. ERdj5 is required as a disulfide reductase for degradation of misfolded proteins in the ER. Science 2008;321:569–72.
[64] Johnson CM, Bortnick SJ, Crawford PC, Papadi GP. Unique susceptibility of the fetal thymus to feline immunodeficiency virus infection: an animal model for HIV infection *in utero*. Am J Reprod Immunol 2001;45:273–88.
[65] Muller JG, Krenn V, Czub S, Stahl-Hennig C, Coulibaly C, Hunsmann G, et al. The thymic epithelial reticulum and interdigitating cells in SIV-induced thymus atrophy and its comparison with other forms of thymus involution. Res Virol 1993;144:93–8.
[66] Aiuti F, Mezzaroma I. Failure to reconstitute $CD4^+$ T-cells despite suppression of HIV replication under HAART. AIDS Rev 2006;8:88–97.
[67] Goldberg GL, Zakrzewski JL, Perales MA, van den Brink MR. Clinical strategies to enhance T cell reconstitution. Semin Immunol 2007;19:289–96.
[68] van den Brink MR, Alpdogan O, Boyd RL. Strategies to enhance T-cell reconstitution in immunocompromised patients. Nat Rev Immunol 2004;4:856–67.
[69] Butorov IV, Nikolenko IA, Butorov SI. Efficacy of galavit in patients with duodenal ulcer. Klin Med (Mosk) 2005;83:72–5.
[70] Nelyubov MV. Cytokins in the pathogenesis of astrakhan spotted fever and North Asian scrub typhus: problems of immunocorrection. Bull Exp Biol Med 2002;134:165–7.
[71] Shaplygin LV, Klopot AM. The efficiency of the drug "Galavit" in complex treatment for infectious and inflammatory diseases of the urogenital system. Voen Med Zh 2006;327:29–34.
[72] Sukhorukov AL. Galavit efficiency in prophylaxis and treatment of pyoinflammatory complications at abdominal surgical pathology. Voen Med Zh 2005;326:31–3.
[73] Vyshegurov I, Anikhovskaia IA, Batmanov Iu E, Iakovlev M. Intestinal endotoxin in the pathogenesis of ocular inflammatory diseases and the antiendoxin constituent of its treatment. Patol Fiziol Eksp Ter 2007:12–4.
[74] Prasad G, Stoica G, Wong PKY. The role of the thymus in the pathogenesis of hind-limb paralysis induced by *ts*1, a mutant of Moloney murine leukemia virus—TB. Virology 1989;169:332–40.
[75] Crise B, Buonocore L, Rose JK. CD4 is retained in the endoplasmic reticulum by the human immunodeficiency virus type 1 glycoprotein precursor. J Virol 1990;64:5585–93.
[76] Li Y, Luo L, Thomas DY, Kang CY. The HIV-1 Env protein signal sequence retards its cleavage and down-regulates the glycoprotein folding. Virology 2000;272:417–28.
[77] Koga Y, Sasaki M, Nskamura K. Intracellular distribution of the envelope glycoprotein of human immunodeficiency virus type 1 and its role in the production of cytopathic effect in $CD4^+$ and $CD4^-$ human cell lines. J Virol 1990;46:4661–71.
[78] Land A, Zonneveld D, Braakman I. Folding of HIV-1 envelope glycoprotein involves extensive isomerization of disulfide bonds and conformation-dependent leader peptide cleavage. FASEB J 2003;17:1058–67.
[79] Aukrust P, Svardal AM, Muller F, Lunden B, Berge RK, Ueland PM, et al. Increased levels of oxidized glutathione in $CD4^+$ lymphocytes associated with disturbed intracellular redox balance in human immunodeficiency virus type 1 infection. Blood 1995;86:258–67.

[80] Aukrust P, Muller F, Svardal AM, Ueland T, Berge RK, Froland SS. Disturbed glutathione metabolism and decreased antioxidant levels in human immunodeficiency virus-infected patients during highly active antiretroviral therapy-potential immunomodulatory effects of antioxidants. J Infect Dis 2003;188:232–8.
[81] Baier-Bitterlich G, Wachter H, Fuchs D. Oxidative stress and apoptosis in HIV infection. Science 1996;271:582–3.
[82] Baruchel S, Wainberg MA. The role of oxidative stress in disease progression in individuals infected by the human immunodeficiency virus. J Leukoc Biol 1992;52:111–4.
[83] Cayota A, Vuillier F, Gonzalez G, Dighiero G. In vitro antioxidant treatment recovers proliferative responses of anergic $CD4^+$ lymphocytes from human immunodeficiency virus-infected individuals. Blood 1996;87:4746–53.
[84] Dobmeyer TS, Findhammer S, Dobmeyer JM, Klein SA, Raffel B, Hoelzer D, et al. Ex vivo induction of apoptosis in lymphocytes is mediated by oxidative stress: role for lymphocyte loss in HIV infection. Free Radic Biol Med 1997;22:775–85.
[85] Gil L, Martinez G, Gonzalez I, Tarinas A, Alvarez A, Giuliani A, et al. Contribution to characterization of oxidative stress in HIV/AIDS patients. Pharmacol Res 2003;47:217–24.
[86] Gulow K, Kaminski M, Darvas K, Suss D, Li-Weber M, Krammer PH. HIV-1 transactivator of transcription substitutes for oxidative signaling in activation-induced T cell death. J Immunol 2005;174:5249–60.
[87] Karamchand L, Dawood H, Chuturgoon AA. Lymphocyte mitochondrial depolarization and apoptosis in HIV-1-infected HAART patients. J Acquir Immune Defic Syndr 2008;48:381–8.
[88] Losa GA, Graber R. Spontaneous apoptosis, oxidative status and immunophenotype markers in blood lymphocytes of AIDS patients. Anal Cell Pathol 2000;21:11–20.
[89] Moretti S, Famularo G, Marcellini S, Boschini A, Santini G, Trinchieri V, et al. L-carnitine reduces lymphocyte apoptosis and oxidant stress in HIV-1-infected subjects treated with zidovudine and didanosine. Antioxid Redox Signal 2002;4:391–403.
[90] Perl A, Banki K. Genetic and metabolic control of the mitochondrial transmembrane potential and reactive oxygen intermediate production in HIV disease. Antioxid Redox Signal 2000;2:551–73.
[91] Piette J, Legrand-Poels S. HIV-1 reactivation after an oxidative stress mediated by different reactive oxygen species. Chem Biol Interact 1994;91:79–89.
[92] Sandstrom PA, Roberts B, Folks TM, Buttke TM. HIV gene expression enhances T cell susceptibility to hydrogen peroxide-induced apoptosis. AIDS Res Hum Retroviruses 1993;9:1107–13.
[93] Sappey C, Legrand-Poels S, Best-Belpomme M, Favier A, Rentier B, Piette J. Stimulation of glutathione peroxidase activity decreases HIV type 1 activation after oxidative stress. AIDS Res Hum Retroviruses 1994;10:1451–61.
[94] Burckhardt CJ, Greber UF. Redox rescues virus from ER trap. Nat Cell Biol 2008;10:9–11.
[95] Popa I, Zubkova I, Medvedovic M, Romantseva T, Mostowski H, Boyd R, et al. Regeneration of the adult thymus is preceded by the expansion of $K5^+K8^+$ epithelial cell progenitors and by increased expression of Trp63, cMyc and Tcf3 transcription factors in the thymic stroma. Int Immunol 2007;19:1249–60.
[96] Ribeiro RM, de Boer RJ. The contribution of the thymus to the recovery of peripheral naive T-cell numbers during antiretroviral treatment for HIV infection. J Acquir Immune Defic Syndr 2008;49:1–8.
[97] Scofield VL, Yan MS, Kuang X, Kim SJ, Wong PKY. The drug monosodium luminol (GVT) preserves crypt-villus epithelial organization and allows survival of intestinal T cells in mice infected with the *ts*1 retrovirus. Immunol Lett 2009, this issue.